Nanoscale

ROYAL SOCIETY OF CHEMISTRY

PAPER

Cite this: *Nanoscale*, 2020, **12**, 24259

Ultra-stretchable supercapacitors based on biaxially pre-strained super-aligned carbon nanotube films†

Yang Yu,[a,b] Zhenhan Fang,[a,c] Yufeng Luo,[a,b] Hengcai Wu,[a] Qunqing Li,[a,c] Shoushan Fan[a,c] and Jiaping Wang *[a,c]

Super-aligned carbon nanotube (SACNT) films with wrinkled structures are prepared by a biaxial pre-strain method and can withstand repetitive stretching of large strains in multiple directions. Ultra-stretchable supercapacitors were fabricated with the SACNT film and active carbon (AC) powders. The initial specific capacitance without strain and with 150% strains in the *X*, *Y* and 45° axes was 91, 88, 89 and 90 F g^{-1}, respectively. Moreover, the capacitance retentions were 97%, 98.5% and 98.6% after 2000 tensile cycles at 0–150% strain in the *X*, *Y* and 45° axes, respectively, demonstrating the excellent strain durability of the SACNT/AC supercapacitors. The stretchable circuit with the combination of stretchable SACNT/AC supercapacitors and SACNT conductors demonstrates a promising method in developing self-contained stretchable functional devices for a variety of applications. The low-cost and scalable biaxial pre-strain process presents a potential route for designing high performance stretchable electronic and energy storage devices.

Received 11th September 2020,
Accepted 17th November 2020

DOI: 10.1039/d0nr06576e

rsc.li/nanoscale

Introduction

The rapid growth of wearable and implantable devices has created a boom in the development of high performance stretchable materials and electronics, which can maintain normal functions and reliability under large deformation.[1–5] Various stretchable electronic devices have been developed for different applications, including stretchable circuits, loudspeakers, pressure and strain sensors, transistors, epidermal electronics, and implantable medical devices.[6–20] As an indispensable component, energy storage devices that are able to deform together with the stretchable systems have attracted much attention. Lithium-ion battery systems with high energy density, high output voltage, and no memory effect are one of the suitable candidates for flexible energy storage devices.[21–23] However, lithium-ion batteries suffer from safety hazards, short lifetime, and low power density. Apart from lithium-ion batteries, supercapacitors have become irreplaceable by virtue of their excellent power density and extremely long operating life, and have increasingly become an attractive candidate for flexible energy storage devices.[24] Many stretchable supercapacitors have been reported in the literature.[25–30] Carbon nanotube (CNT) is considered as a promising material for use in stretchable supercapacitors because of its high specific surface area, large aspect ratio, mechanical robustness, and excellent electrical conductivity.[31,32] Stretchable supercapacitors based on buckled single-walled CNT (SWCNT) macrofilms are able to stand about 30% strain without performance degradation.[33] Integrated supercapacitors based on SWCNT films with reticulate architecture can maintain their properties at strain as high as 120%.[34] However, the existing stretchable supercapacitors using CNTs as electrodes only demonstrate stretchability at uniaxial strain, which limits their practical applications in implantable or wearable devices embedded in soft and elastic biological tissue, where the devices are mostly stretched in different directions. Therefore, developing high-performance stretchable supercapacitors that can withstand large and repeated strain in different axes becomes critical.

Super-aligned CNTs (SACNTs) have attracted much attention these years.[35,36] Unlike regular CNTs, SACNTs have very clean surfaces and extremely large aspect ratio. Ultrathin and continuous SACNT films are drawn from SACNT arrays using a cost-effective and environmentally benign method by an end-to-end joining mechanism and can be stacked together to achieve isotropic electrical conductivity. The SACNT films are freestanding, light weight, and possess excellent electrical and mechanical properties along their axial direction and have

[a]*Department of Physics and Tsinghua-Foxconn Nanotechnology Research Center, Tsinghua University, Beijing, China. E-mail: jpwang@tsinghua.edu.cn*
[b]*School of Materials Science and Engineering, Tsinghua University, Beijing, China*
[c]*Frontier Science Center for Quantum Information, Beijing, China*
†Electronic supplementary information (ESI) available. See DOI: 10.1039/d0nr06576e

demonstrated a variety of applications such as loudspeakers and stretchable conductors.[37,38] By compositing the films with other materials, the SACNT films have been widely used for the development of high-performance electrodes for various kinds of high performance and stretchable energy storage devices.[39–46]

Herein, a low-cost and scalable biaxial pre-strain process was used to fabricate ultra-stretchable SACNT/active carbon (AC) supercapacitor and SACNT conductive films. The stretchable SACNT film could withstand high and repeated strains in different axes without large conductivity decay. Stretchable supercapacitors assembled with the stretchable SACNT films and AC powders demonstrated unprecedented stretchability and high capacitive performance at high strains in different axes. Stable capacitive charge–discharge behaviors were also demonstrated during tensile cycles. Moreover, stretchable circuits consisting of stretchable SACNT/AC supercapacitors and SACNT conductors represent a promising direction in developing self-contained stretchable devices for a wide range of applications.

Experimental

Preparation of the SACNT film and the polydimethylsiloxane (PDMS) substrate

SACNT arrays with a tube diameter of 20–30 nm and a height of 300 μm were synthesized on silicon wafers by chemical vapor deposition. Details of the synthesis method are reported in previous papers[47,48] Continuous SACNT films were directly drawn from the SACNT arrays. PDMS substrates with a thickness of 1 mm were prepared by mixing the base and the curing agent at a weight ratio of 10 : 1 using Sylgard 184 (Dow Corning). The mixture was cured at 70 °C for 1 h. After cooling down to room temperature, the PDMS substrates were cut into 60 mm × 60 mm pieces, and their optical photograph is shown in Fig. S1.†

Fabrication of the stretchable SACNT composites

Fig. 1a shows the schematic of the fabrication process of the stretchable SACNT conductors and SACNT/AC supercapacitor electrodes. First, a PDMS square substrate with a length L was biaxially pre-strained in two perpendicular directions to $L + \Delta L$ (Fig. S1†), and covered with a cross-stacked 6-layer SACNT film. Then, a thin polyethylene (PE) film with two rectangular openings with a dimension of 10 mm × 20 mm was stacked on top of the SACNT film as a mask for making supercapacitor electrodes. 45 mg of AC powder (XFP01, XF Chem Co., Ltd, specific surface area: 2000 $m^2\ g^{-1}$) was dispersed in 60 mL of ethanol by ultrasonication for 45 minutes. The suspension of AC powder in ethanol was dropped on the mask with a pipette. After the evaporation of ethanol and the removal of the mask, the AC powder only existed in the exposed area through the rectangular openings of the mask. A cross-stacked 2-layer SACNT film was coated on top of the SACNT film and AC powder, followed by the processes of stacking the PE mask and dropping the AC suspension, which were repeated 20 times. Afterwards, another cross-stacked 6-layer SACNT film was stacked on top of the composite film, forming a composite film consisting of a SACNT/AC sandwich structure in the areas of the rectangular openings and pure SACNT film in the remaining part. After the pre-strained PDMS substrate was released to its original length L, a stretchable SACNT conductor and a SACNT/AC supercapacitor electrode were fabricated. The areal density of the supercapacitor electrodes was 5 mg cm^{-2}. The weight ratio of AC in the SACNT/AC composite electrode was larger than 95%. The stretchable composite films with the SACNT/AC and the pure SACNT areas were then laser cut to different patterns to assemble stretchable circuits (Fig. 1b). The size of the SACNT/AC composite electrodes was 10 mm × 20 mm.

Preparation of the gel electrolyte and assembly of the stretchable supercapacitors

The gel electrolyte was prepared by dissolving 0.60 g of polyvinyl alcohol (PVA, Sinopharm Chemical Reagent Co., Ltd) and 0.60 g of 1 M H_3PO_4 (Sinopharm Chemical Reagent Co., Ltd) in 6 mL of DI water at 80 °C with stirring for 5 hours. The gel electrolyte was then dropped on an SACNT/AC composite electrode and dried at 70 °C for 1 h. Two SACNT/AC composite electrodes with the gel electrolyte were stacked together and uncured PDMS paste was used to seal the package. After curing of the PDMS, a stretchable SACNT/AC supercapacitor was fabricated. Herein, two SACNT/AC supercapacitors were connected by the SACNT conductor. The gel electrolyte was used to accommodate any deformation of the stretchable electrodes (Fig. 1c). Photograph of a light emitting diode (LED) illuminated by the stretchable circuit is shown in Fig. 1d.

Characterization methods

The resistances of the SACNT/AC composites at strains up to 150% were characterized. The dimensions of the sample were 70 mm × 10 mm × 0.6 mm. Two copper foils were attached at both ends of the sample by conductive silver paste for resistance measurements. A tensile load was applied using an Instron 5848 microtester and the resistances of the SACNT composite electrodes were monitored by a Keithley 2400 Source Meter. The durability of the stretchable supercapacitors was characterized by performing 2000 cyclic tensile tests at 0–150% strains and the electrochemical properties of the composites were tested using a Land battery test system (Wuhan Land Electronic Co., China) with a cut-off voltage of 0–1 V. Cyclic voltammetry (CV) curves were measured in a voltage window of 0–1 V at a scan rate of 100 mV s^{-1}.

Results and discussion

Morphology and resistance changes of the SACNT/AC electrodes

Fig. S1† illustrates that AC powders were uniformly dispersed on the cross-stacked SACNT films, maintaining an excellent

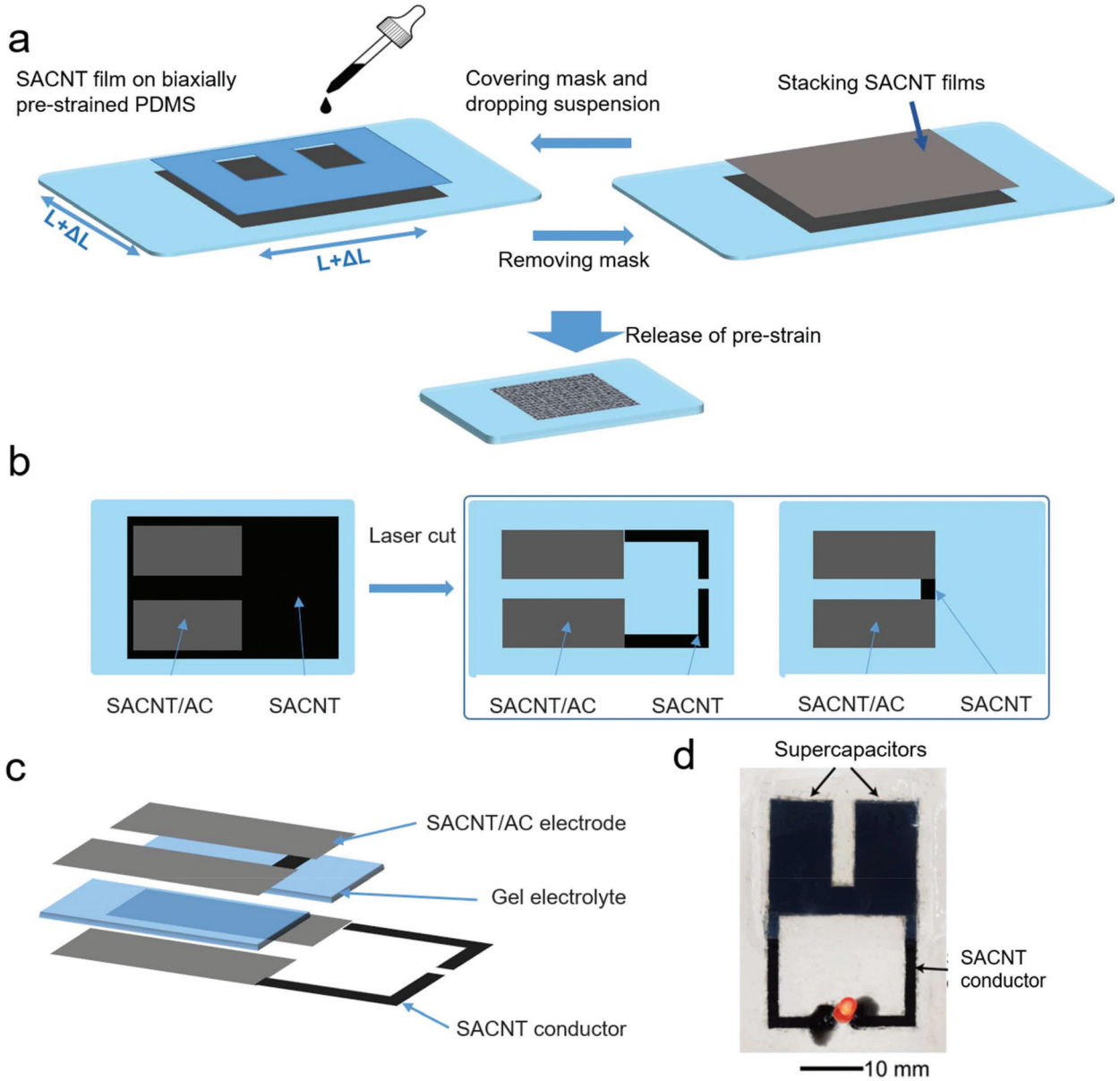

Fig. 1 (a) Schematic of the process for fabricating stretchable supercapacitor electrodes and conductor films. (b) Supercapacitor electrodes and conductors before and after laser cut. (c) Schematic of the structures of stretchable supercapacitors and conductors. (d) Photograph of an LED powered by a stretchable circuit consisting of the SACNT/AC supercapacitor and SACNT conductor.

conductive structure. Fig. 2a and b show SEM images of an SACNT/AC composite electrode and an SACNT conductor. Wrinkled structures were observed on both surfaces, which formed during the pre-strain and release process. Similar wrinkled structures on the surface of CNT composite electrodes for use in stretchable lithium ion batteries were also reported in our previous paper.[49]

Fig. 3 shows the normalized resistance changes ($\Delta R/R_0$) of the SACNT/AC composite electrodes with and without pre-strain as a function of applied strain in different axes (*X*, *Y*, 30°, and 45°). The resistance of the composite electrode without pre-strain increased sharply as the applied strain increased. The normalized resistance increased by 50% at 35% strain in the *X* axis, which would impair the electrochemical performance of the electrode. The composite electrodes with 150% biaxial pre-strain showed more stable resistance at applied strains up to 150% in different tensile axes. The normalized resistances of the biaxially pre-strained electrodes increased by 6.2%, 6%, 5.1%, and 5.9% at 150% strain in the *X*, *Y*, 30°, and 45° axes, respectively. The low resistance changes of the composite electrodes were ascribed to the wrinkled structures on the surface that can extend along the strain axis to prevent the CNT composite structures from fracture and maintain stable electrical properties. The pre-strained

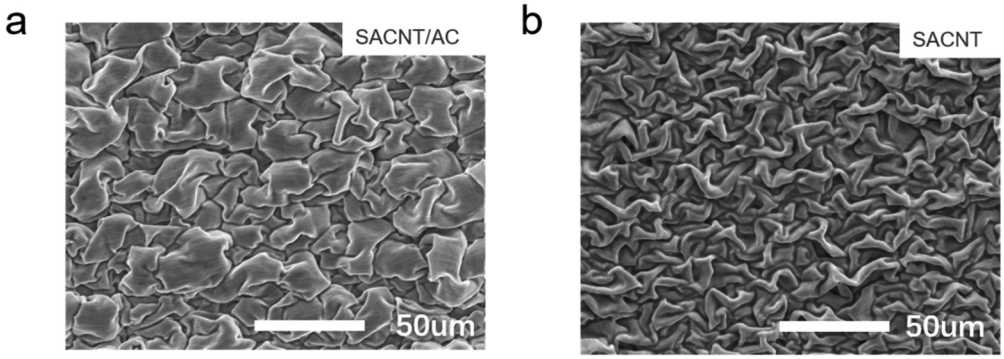

Fig. 2 SEM images of the pre-strained (a) SACNT/AC electrode and (b) SACNT conductor.

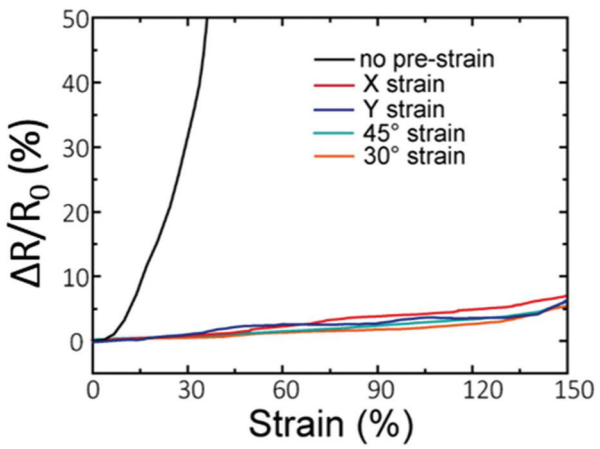

Fig. 3 Normalized resistance changes of an SACNT/AC supercapacitor electrode at applied strain up to 150% along different directions.

SACNT/AC composites demonstrate potential for use in high-performance stretchable devices.

Electrochemical properties of the SACNT/AC supercapacitors

To demonstrate the stretchability and performance of the SACNT/AC supercapacitors, their CV and galvanostatic charge/discharge behaviors were tested. Fig. 4a and b present the CV curves of the SACNT/AC supercapacitors with and without strains in different axes. All the curves exhibit a typical rectangular shape at a scan rate of 100 mV s^{-1}, indicating the behavior of an ideal double-layer electrochemical capacitor. In addition, no significant change was observed in the CV cures of the supercapacitors when they were either uniaxially strained to 150% in different axes (*X*, *Y*, and 45°, Fig. 4a) or biaxially strained to 150% × 150% (*X*–*Y*, Fig. 4b), demonstrating the stable performances of the stretchable SACNT/AC supercapacitor at uniaxial and biaxial strains as high as 150%.

Fig. 4c shows the galvanostatic charge–discharge curves of the SACNT/AC supercapacitors with no strain and with 150% strains in different axes (*X*, *Y*, 45°, and *X*–*Y*) at a constant current density of 1 A g^{-1}. These charge–discharge curves almost overlapped together, suggesting that the SACNT/AC supercapacitors can withstand extremely large deformation either uniaxially or biaxially. The cycling stability of the stretchable SACNT/AC supercapacitors subjected to 150% strains in different axes was illustrated by the galvanostatic charge–discharge test at a current density of 1 A g^{-1} up to 1000 cycles. Fig. 4d shows the specific capacitances of the single SACNT/AC supercapacitors with and without strains. The initial specific capacitances without strain and with 150% strains in *X*, *Y*, and 45° axes were 91, 88, 89, and 90 F g^{-1}, respectively. Remarkably, the specific capacitances of the SACNT/AC supercapacitors with or without strains remained unchanged for up to 1000 charge–discharge cycles, demonstrating their excellent electrochemical stability under large deformation.

Strain durability of the SACNT/AC supercapacitors was tested by carrying out electrochemical characterization under large deformation in different axes for 2000 tensile cycles. Fig. 4e shows the capacitance retentions of the SACNT/AC supercapacitors during 2000 tensile cycles at 0–150% strains in different axes. Only slight capacitance degradation was observed. The capacitance retentions were 97%, 98.5%, and 98.6% after 2000 tensile cycles at 0–150% strains in the *X*, *Y*, and 45° axes, proving excellent strain durability of the SACNT/AC supercapacitors. Fig. 4f shows the galvanostatic charge–discharge curves of the SACNT/AC supercapacitors at 0.5 A g^{-1} during cyclic tensile cycles with 150% strains in different axes at a high strain rate of 7.5% strain s^{-1}. The charge–discharge curves remained as straight lines when the dynamic tensile cycles were applied in *X*, *Y*, and 45° axes. The reproducible and stable capacitive behavior of the SACNT/AC supercapacitors shows that the *in situ* applied stretching/releasing processes had no significant effect on the charge–discharge feature of the sample and proves that the stretchable supercapacitors can be reversibly charged and discharged during tensile cycles with a high strain rate in different axes. These results demonstrate outstanding stretchability and durability of the biaxially pre-strained SACNT/AC supercapacitors under applied high strains in different axes, proving the biaxial pre-strain process as a promising method for fabricating ultra-stretchable and high-performance supercapacitors.

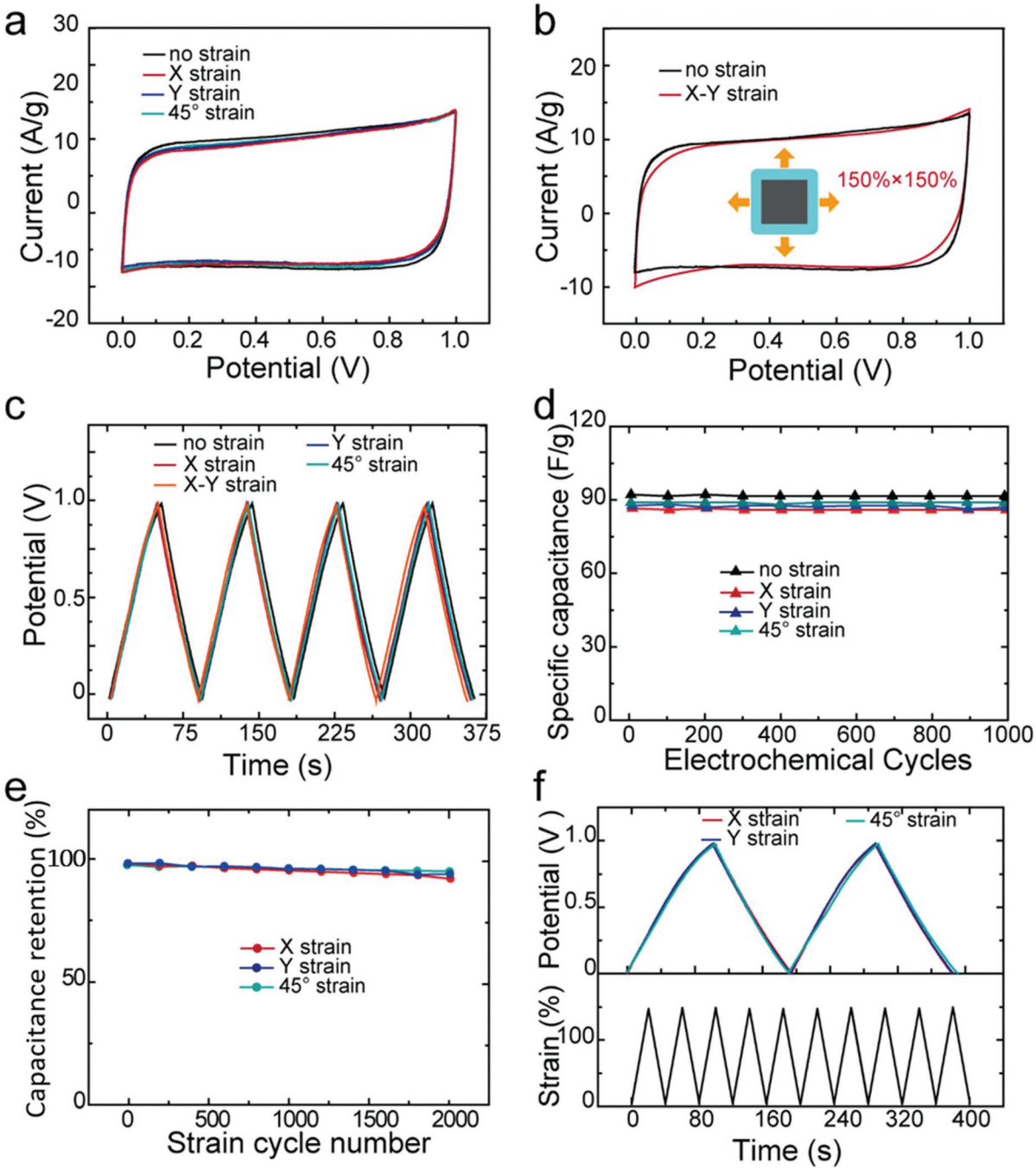

Fig. 4 CV curves of the SACNT/AC supercapacitor (a) with no strain and with strains in *X*, *Y*, and 45° axes and (b) with no strain and with *X*–*Y* strain, measured at a scan rate of 100 mV s^{-1}. (c) Galvanostatic charge–discharge curves and (d) cycling performances of the SACNT/AC supercapacitors with and without 150% strain in different axes. (e) Capacitance retention of the SACNT supercapacitor during 2000 tensile cycles under 150% strains in *X*, *Y*, and 45° axes. (f) Galvanostatic charge–discharge curves of the SACNT supercapacitor during stretching/releasing processes at 150% strain in *X*, *Y*, and 45° axes.

Finally, an LED was illuminated by a stretchable circuit consisting of the SACNT/AC supercapacitor and the CNT conductor, as shown in Fig. 5a. When the circuit was stretched to approximately 100% in both *X* and *Y* directions, the LED did not show any noticeable luminance change (Fig. 5b). Even when the biaxially stretched circuit was further pressed by a finger, the LED still functioned well (Fig. 5c), demonstrating the ultra-stretchability of the biaxially pre-strained circuit and presenting great potential for the development of high performance stretchable electronic devices.

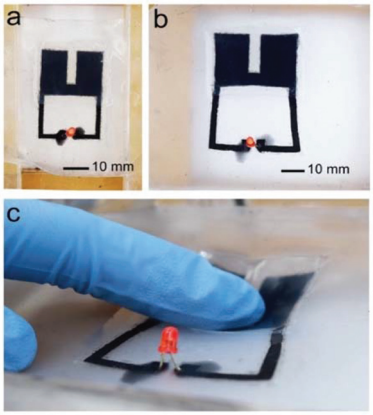

Fig. 5 An LED powered by a stretchable circuit consisting of the SACNT/AC supercapacitor and SACNT conductor. (a) no strain, (b) *X*–*Y* stain, (c) pressed by a finger.

Conclusions

Ultra-stretchable SACNT/AC composite electrodes were fabricated by forming wrinkled structures on the surface of SACNT/AC films using a biaxial pre-strain process. Stretchable supercapacitors were assembled with the stretchable composite electrodes and gel electrolyte, which demonstrated unprecedented stretchability, reliability, and high capacitive performance at high strain in different axes. The stretchable circuit with the integration of stretchable supercapacitors and conductors represents a promising direction in developing self-contained stretchable functional devices for a wide range of applications. In addition, the low-cost and scalable biaxial pre-strain process paves a way for designing high performance stretchable electronic and energy-storage devices.

Conflicts of interest

There are no conflicts to declare.

Acknowledgements

This work was supported by the National Basic Research Program of China (2019YFA0705702) and the National Natural Science Foundation of China (51872158 and 51532008).

Notes and references

1 B. Y. Ahn, E. B. Duoss, M. J. Motala, X. Guo, S.-I. Park, Y. Xiong, J. Yoon, R. G. Nuzzo, J. A. Rogers and J. A. Lewis, *Science*, 2009, **323**, 1590–1593.
2 J. Kim, G. A. Salvatore, H. Araki, A. M. Chiarelli, Z. Xie, A. Banks, X. Sheng, Y. Liu, J. W. Lee, K.-I. Jang, S. Y. Heo, K. Cho, H. Luo, B. Zimmerman, J. Kim, L. Yan, X. Feng, S. Xu, M. Fabiani, G. Gratton, Y. Huang, U. Paik and J. A. Rogers, *Sci. Adv.*, 2016, **2**(8), e1600418.
3 X. Yu, Z. Xie, Y. Yu, J. Lee, A. Vazquezguardado, H. Luan, J. Ruban, X. Ning, A. Akhtar, D. Li, B. Ji, Y. Liu, R. Sun, J. Cao, Q. Huo, Y. Zhong, C. M. Lee, S. Y. Kim, P. Gutruf, C. Zhang, Y. Xue, Q. Guo, A. Chempakasseril, P. Tian, W. Lu, J. Y. Jeong, Y. J. Yu, J. Cornman, C. S. Tan, B. H. Kim, K. H. Lee, X. Feng, Y. Huang and J. A. Rogers, *Nature*, 2019, **575**, 473–479.
4 J. A. Rogers, T. Someya and Y. G. Huang, *Science*, 2010, **327**, 1603–1607.
5 D. Y. Khang, H. Q. Jiang, Y. Huang and J. A. Rogers, *Science*, 2006, **311**, 208–212.
6 D.-H. Kim, J.-H. Ahn, W. M. Choi, H.-S. Kim, T.-H. Kim, J. Song, Y. Y. Huang, Z. Liu, C. Lu and J. A. Rogers, *Science*, 2008, **320**, 507–511.
7 S. P. Lacour, S. Wagner, Z. Huang and Z. Suo, *Appl. Phys. Lett.*, 2003, **82**, 2404–2406.
8 T. Sekitani, Y. Noguchi, K. Hata, T. Fukushima, T. Aida and T. J. S. Someya, *Science*, 2008, **321**, 1468–1472.
9 T. Sekitani, H. Nakajima, H. Maeda, T. Fukushima, T. Aida, K. Hata and T. Someya, *Nat. Mater.*, 2009, **8**, 494–499.
10 F. Xu and Y. Zhu, *Adv. Mater.*, 2012, **24**, 5117–5122.
11 C. Keplinger, J. Sun, C. C. Foo, P. Rothemund, G. M. Whitesides and Z. Suo, *Science*, 2013, **341**, 984–987.
12 L. Xiao, Z. Chen, C. Feng, L. Liu, Z. Bai, Y. Wang, L. Qian, Y. Zhang, Q. Li, K. Jiang and S. Fan, *Nano Lett.*, 2008, **8**, 4539–4545.
13 L. Xiao, Z. Chen, C. Feng, L. Liu, Z. Bai, Y. Wang, L. Qian, Y. Zhang, Q. Li, K. Jiang and S. Fan, *Nano Lett.*, 2012, **12**, 2652–2652.
14 G. Ge, Y. Zhang, J. Shao, W. Wang, W. Si, W. Huang and X. Dong, *Adv. Funct. Mater.*, 2018, **28**, 1802576.
15 T. Yamada, Y. Hayamizu, Y. Yamamoto, Y. Yomogida, A. Izadinajafabadi, D. N. Futaba and K. Hata, *Nat. Nanotechnol.*, 2011, **6**, 296–301.
16 M. Amjadi, A. Pichitpajongkit, S. Lee, S. Ryu and I. Park, *ACS Nano*, 2014, **8**, 5154–5163.
17 J. Lee, S. Kim, J. Lee, D. Yang, B. C. Park, S. Ryu and I. Park, *Nanoscale*, 2014, **6**, 11932–11939.
18 S. K. Lee, B. J. Kim, H. Jang, S. C. Yoon, C. Lee, B. Hong, J. A. Rogers, J. H. Cho and J. H. Ahn, *Nano Lett.*, 2011, **11**, 4642–4646.
19 A. Chortos, J. Lim, J. W. F. To, M. Vosgueritchian, T. J. Dusseault, T. Kim, S. Hwang and Z. Bao, *Adv. Mater.*, 2014, **26**, 4253–4259.
20 J. Y. Oh, S. Rondeaugagne, Y. Chiu, A. Chortos, F. Lissel, G. N. Wang, B. C. Schroeder, T. Kurosawa, J. Lopez and T. Katsumata, *Nature*, 2016, **539**, 411–415.
21 Z. H. Fang, J. Wang, H. Wu, Q. Q. Li, S. S. Fan and J. P. Wang, *J. Power Sources*, 2020, **454**, 227932.
22 Y. Huang, H. Yang, T. Xiong, D. Adekoya, W. Qiu, Z. Wang, S. Zhang and M. S. Balogun, *Energy Storage Mater.*, 2020, **25**, 41–51.
23 T. Xiong, H. Su, F. Yang, Q. Tan, P. B. S. Appadurai, A. A. Afuwape, K. Guo, Y. Huang, Z. Wang and M. S. Balogun, *Mater. Today Energy*, 2020, **17**, 100461.

24 P. Simon and Y. Gogotsi, *Nat. Mater.*, 2008, **7**, 845–854.
25 L. Hu, M. Pasta, F. La Mantia, L. Cui, S. Jeong, H. D. Deshazer, J. W. Choi, S. M. Han and Y. Cui, *Nano Lett.*, 2010, **10**, 708–714.
26 Z. Yang, J. Deng, X. Chen, J. Ren and H. Peng, *Angew. Chem., Int. Ed.*, 2013, **52**, 13453–13457.
27 Y. Huang, M. Zhong, Y. Huang, M. Zhu, Z. Pei, Z. Wang, Q. Xue, X. Xie and C. Zhi, *Nat. Commun.*, 2015, **6**, 10310–10310.
28 Y. Huang, M. Zhong, F. Shi, X. Liu, Z. Tang, Y. Wang, Y. Huang, H. Hou, X. Xie and C. Zhi, *Angew. Chem., Int. Ed.*, 2017, **56**, 9141–9145.
29 W. Liu, M. Song, B. Kong and Y. Cui, *Adv. Mater.*, 2017, **29**, 1603436.
30 T. Chen, Y. Xue, A. K. Roy and L. Dai, *ACS Nano*, 2014, **8**, 1039–1046.
31 S. Fan, M. Chapline, N. R. Franklin, T. W. Tombler, A. M. Cassell and H. Dai, *Science*, 1999, **283**, 512–514.
32 R. H. Baughman, A. A. Zakhidov and W. A. De Heer, *Science*, 2002, **297**, 787–792.
33 C. Yu, C. Masarapu, J. Rong, B. Wei and H. Jiang, *Adv. Mater.*, 2009, **21**, 4793–4797.
34 Z. Niu, H. Dong, B. Zhu, J. Li, H. H. Hng, W. Zhou, X. Chen and S. Xie, *Adv. Mater.*, 2013, **25**, 1058–1064.
35 K. Jiang, J. Wang, Q. Li, L. Liu, C. Liu and S. Fan, *Adv. Mater.*, 2011, **23**, 1154–1161.
36 K. Jiang, Q. Li and S. Fan, *Nature*, 2002, **419**, 801–801.
37 K. Liu, Y. Sun, P. Liu, X. Lin, S. Fan and K. Jiang, *Adv. Funct. Mater.*, 2011, **21**, 2721–2728.
38 Y. Yu, S. Luo, L. Sun, Y. Wu, K. Jiang, Q. Li, J. Wang and S. Fan, *Nanoscale*, 2015, **7**, 10178–10185.
39 S. Luo, K. Wang, J. Wang, K. Jiang, Q. Li and S. Fan, *Adv. Mater.*, 2012, **24**, 2294–2298.
40 S. Luo, H. Wu, Y. Wu, K. Jiang, J. Wang and S. Fan, *J. Power Sources*, 2014, **249**, 463–469.
41 Y. Luo, N. Luo, W. Kong, H. Wu, K. Wang, S. Fan, W. Duan and J. Wang, *Small*, 2018, **14**, 1702853.
42 D. Wang, K. Wang, H. Wu, Y. Luo, L. Sun, Y. Zhao, J. Wang, L. Jia, K. Jiang and Q. Li, *Carbon*, 2018, **132**, 370–379.
43 K. Wang, S. Luo, Y. Wu, X. He, F. Zhao, J. Wang, K. Jiang and S. J. Fan, *Adv. Funct. Mater.*, 2013, **23**, 846–853.
44 K. Wang, Y. Wu, S. Luo, X. He, J. Wang, K. Jiang and S. S. Fan, *J. Power Sources*, 2013, **233**, 209–215.
45 L. Yan, N. Luo, W. Kong, S. Luo, H. Wu, K. Jiang, Q. Li, S. Fan, W. Duan and J. Wang, *J. Power Sources*, 2018, **389**, 169–177.
46 K. Zhu, Y. Luo, F. Zhao, J. Hou, X. Wang, H. Ma, H. Wu, Y. Zhang, K. Jiang, S. Fan, J. Wang and K. Liu, *ACS Sustainable Chem. Eng.*, 2018, **6**(3), 3426–3433.
47 K. Liu, Y. Sun, L. Chen, C. Feng, X. Feng, K. Jiang, Y. Zhao and S. Fan, *Nano Lett.*, 2008, **8**, 700–705.
48 K. Liu, Y. Sun, P. Liu, X. Lin, S. Fan and K. Jiang, *Adv. Funct. Mater.*, 2011, **21**, 2721–2728.
49 Y. Yu, Y. Luo, H. Wu, K. Jiang, Q. Li, S. Fan, J. Li and J. Wang, *Nanoscale*, 2018, **10**, 19972–19978.